

Novel Methods for Moving Interfaces

David Noble (1541)

SAND2008-4594P

Project Summary

Motivation: Interface physics and dynamics are the controlling phenomena in numerous applications. Efficient, robust interface capturing techniques are required for a predictive capability for these applications.

Objectives: To radically improve our speed and robustness in simulating moving interface problems while accurately capturing the interfacial physics.

- For multiphase flows (fluid-fluid, solid-fluid)
- For phase change

Approach: Develop new discretization/stabilization techniques

- Discretization: Level sets, eXtended Finite Element Methods (XFEM), Conformal Decomposition Finite Element Method (CDFEM)
- Stabilization: MINI element, PPPS Stabilization, Pressure Projection, Pseudo-compressible

Applications: Laser welding, Encapsulation, Nanoparticle suspensions, Ablation

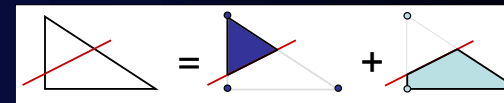


CDFEM Theory

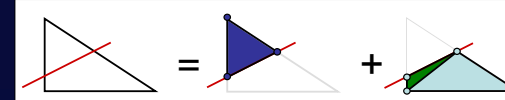
CDFEM Description

- Decompose elements that span the moving interface into conformal elements
- Cross between ALE and Level set methods

XFEM Approximation



CDFEM Approximation

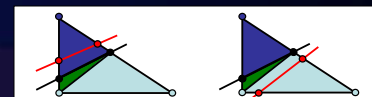


- Identical IFF interfacial nodes in CDFEM are constrained to match XFEM values at nodal locations
- CDFEM space contains XFEM space
- Guaranteed to be at least as accurate

CDFEM Moving Interface Prototype

Cross between ALE and Level Set

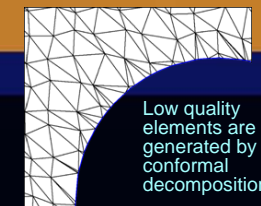
- Must address moving nodes and sign change



Methodology

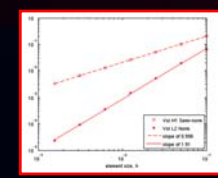
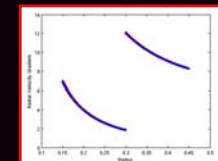
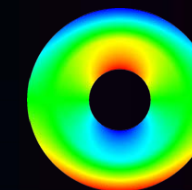
- Use ALE type approach in inertial term
- Consider new nodes to have “adverted” from the nearest existing point on the interface

CDFEM Static Interface Validation



Research Issue

Validation: 2-Phase Annular Couette Flow

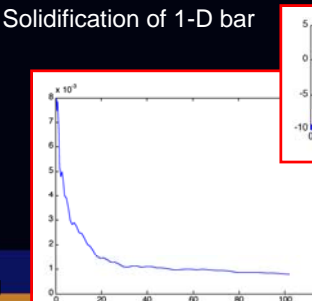
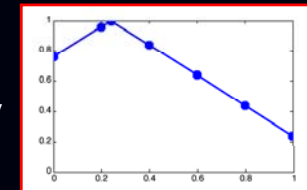


Conclusion:

- Optimal rates of convergence obtained
- Low quality subelements do not adversely impact accuracy norms of the value or gradient

Validation

- Advection of weak discontinuity
 - Exact solution recovered
- Solidification of 1-D bar



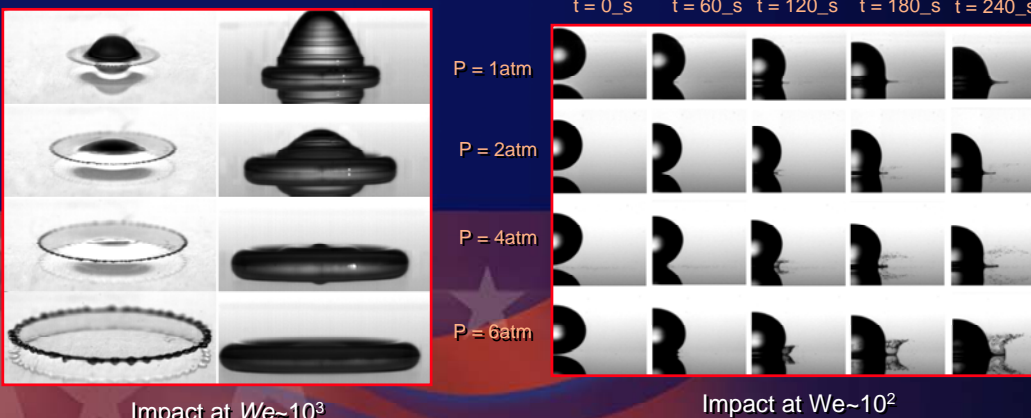
Droplet Impact and Dispersion Physics

Rich Jepsen (1534), Alex Brown (1532)

Investigate the Physics of High-speed liquid Impact, Dispersion and Ignition. Develop models to predict these high consequence events.

LDRD Objectives: Applied Testing, Diagnostics, and Model Development

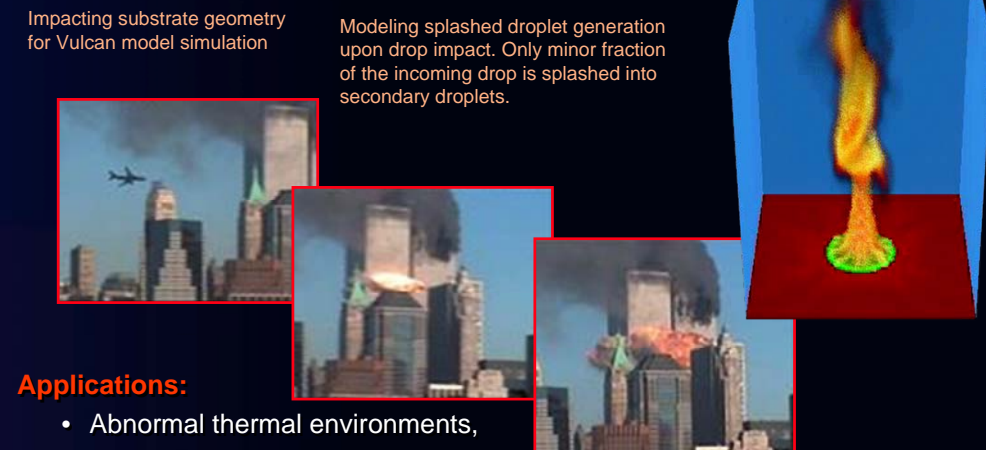
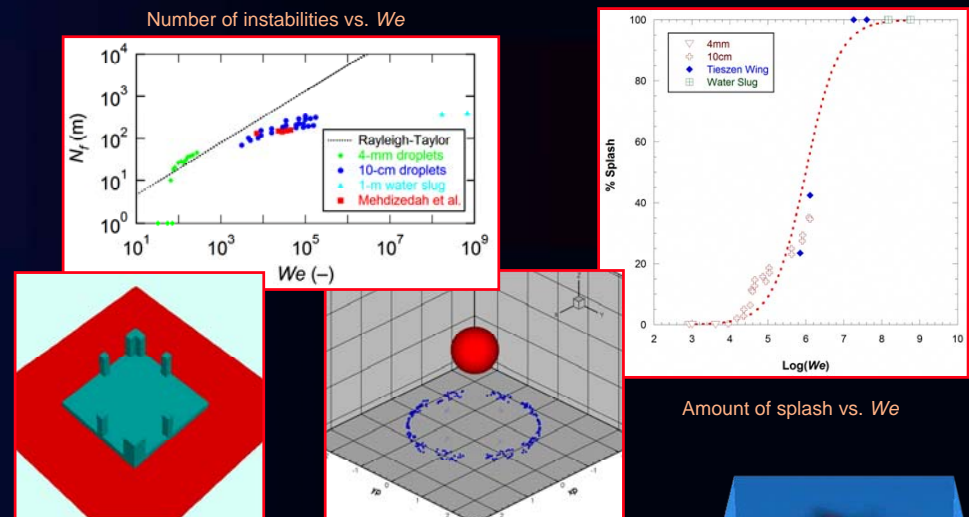
- Utilize Sandia's test facilities to create a large range of impact speed and droplet sizes. Weber number (We) from 10^2 to 10^8
- Dispersion parameters are measured using High-speed video, laser, load cells, and other techniques
- Develop preliminary Computational Fluid Dynamics (CFD) models to describe physics, predict impact and dispersion processes



Impact at $We \sim 10^3$ with increased ambient pressure (1 to 6 atm). Demonstrates effects of ambient air density on splash characteristics.

ESRF Objectives:

- Determine optimal models for a spray modeling capability at Sandia
- Incorporate new findings from LDRD work in new models
- Provide guidance for code merging efforts: CHT/Fire Code Aria/Fuego

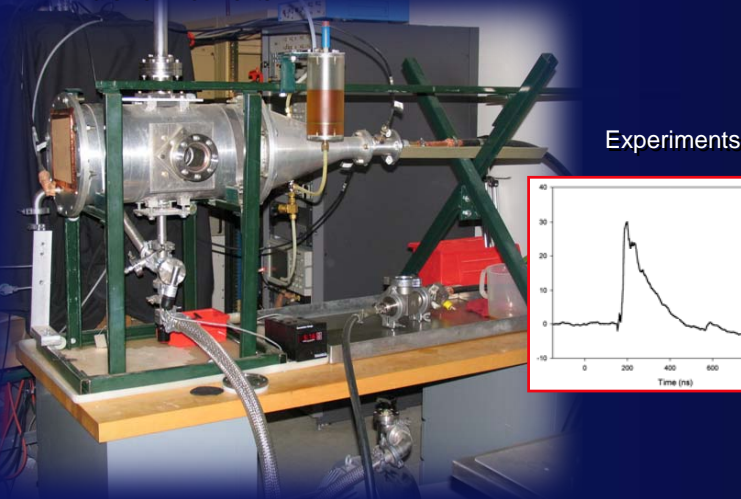


Streamer Initiation in Volume and Surface Discharges in Atmospheric Gases

Jane Lehr (1654) and Roy Jorgenson (1652)

Volumetric Breakdown Experiments in Air and N₂

Use improved understanding of breakdown physics to predict the effect that variations in geometry and environment will have on threshold levels for reliability engineering in electrically harsh environments

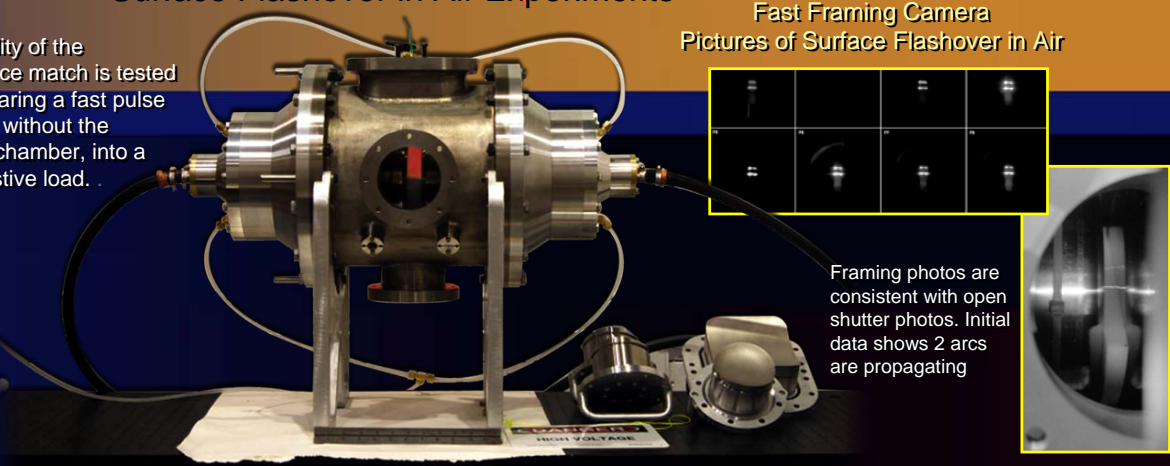


Experiments

The quality of the impedance match is tested by comparing a fast pulse with and without the shorted chamber, into a fast resistive load.

Surface Flashover in Air Experiments

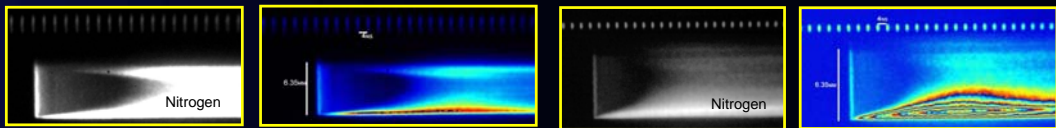
Fast Framing Camera
Pictures of Surface Flashover in Air



Framing photos are consistent with open shutter photos. Initial data shows 2 arcs are propagating

We see Distinct Differences between Air and Nitrogen

Streamer Velocities $\sim 4 \cdot 10^7$ cm/s



Laboratory Air

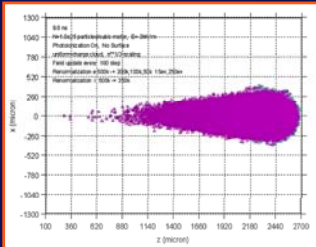
Nitrogen

Nitrogen

Theory and Modeling

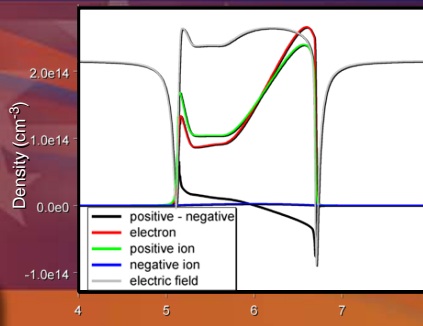
Local 3D simulations

- Monte Carlo (kinetic)
- Air properties
- Photoionization



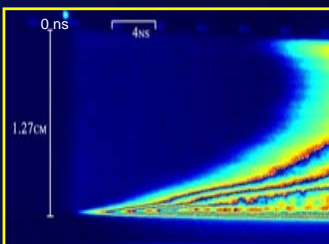
Global 1.5D (Morrow)

- One dimensional, flux corrected transport
- E Field 3d due to discs
- Rates from Monte Carlo

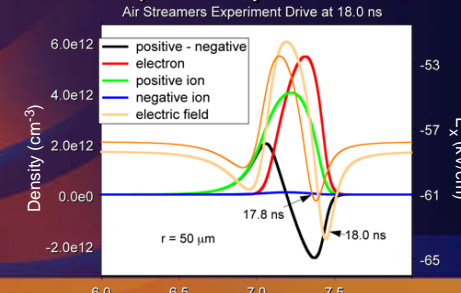


Comparison of Velocities

Measured Velocity = $4 \cdot 10^7$ cm/s



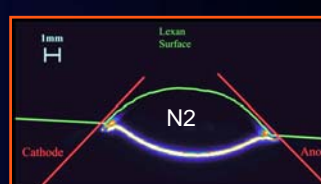
Computed Velocity = $3.5 \cdot 10^7$ cm/s



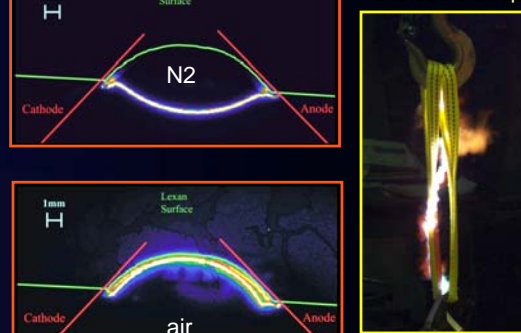
Sandia is a multiprogram laboratory operated by Sandia Corporation, a Lockheed Martin Company, for the United States Department of Energy's National Nuclear Security Administration under contract DE-AC04-94AL85000.

Reasons for Studying Surface Flashover

Texas Tech- Sandia Collaboration



Flashover Across
Dielectric Strap



Arcs may follow field lines or follow dielectric surface depending on dielectric and gas properties - shows importance of surface physics

Summary

- Streamer velocities in atmospheric air are being measured with a fast Streak camera
- Comparisons between experiments and theory are excellent.
- Surface interactions introduced into streamer model and several cases examined at atmospheric pressure
- Sustaining fields are examined with model and will be used to design experiments.
- Surface experimental fixture constructed and initial shots run

Micromechanics Experimental Techniques

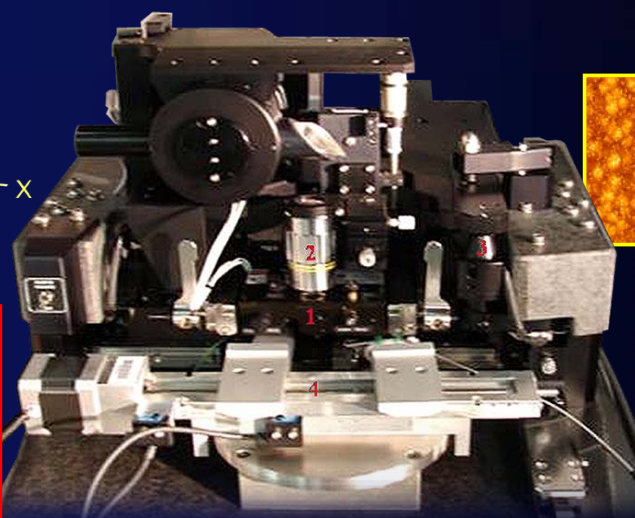
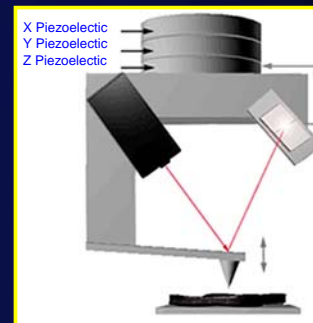
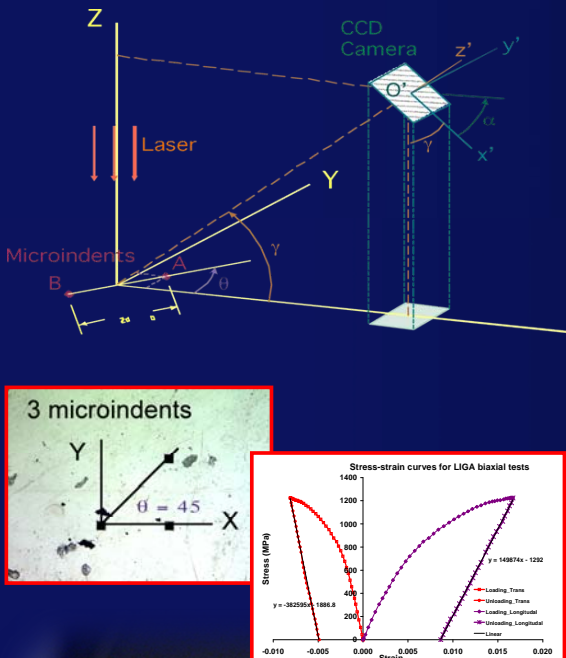
Wei-Yang Lu and Helena Jin, (8776)

• Introduction

- Develop experimental techniques for point/field strain measurements at micro/nano size scale.
- Apply techniques to make measurements and gain fundamental understanding of size effects of materials/structures' deformation/failure.

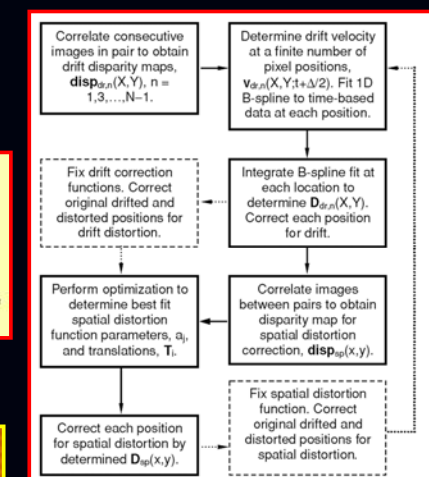
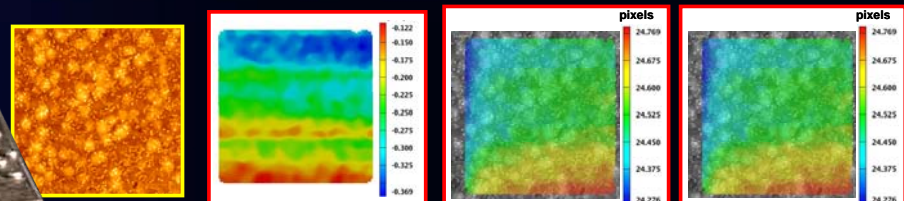
• Multi-Marker Laser Interferometry

- Optical rosette strain gage with gage length less than 150 μm .



• Field Strain Measurement Using AFM Images

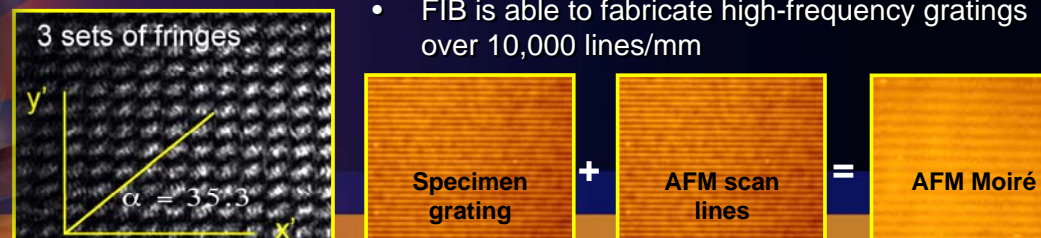
- Calibration of AFM thermal drift and spatial distortion.
- Consecutive scanning to calibrate the thermal drift
 - ideal value should be 0 displacement.
- Incrementally relocate specimen by 0.5 μm to calibrate the spatial drift – ideal displacement should be uniform 25.6 pixels and 51.2 pixels



• AFM Moiré

- measure strain at nanometer scale.

- FIB is able to fabricate high-frequency gratings over 10,000 lines/mm



Predicting Mixing and Reaction with Multiple Sources

John Hewson (1532)

Allowing multi-scale methods for turbulent-reacting flows to solve problems in high-consequence environments

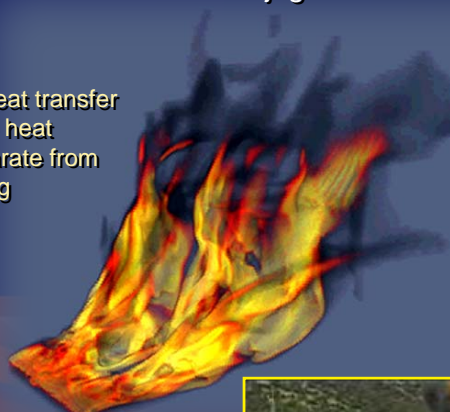
Problem statement

- Turbulent reacting flows of interest are multi-scale problems
 - Device scale determines turbulence scales.
 - Reaction-diffusion scales orders of magnitude smaller.
- Separate models using multi-scale methods
 - Large-scale: CFD transporting conserved scalars.
 - Reaction-diffusion processes referenced to conserved scalars: lookup tables pre-computed for speed
- To date, these methods only applied to two-source mixing.

Application of immediate interest

- Solid-propellant fires: aluminum particles oxidize in solid-propellant products and in ambient air.
- Hydrocarbon fires with conjugate heat transfer.

Issue: wall-heat transfer and radiative heat transfer separate from fuel-air mixing



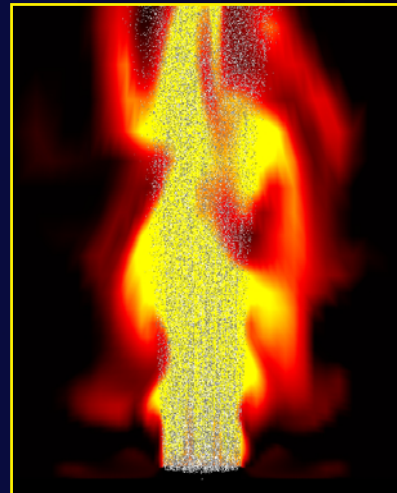
Progress: new subgrid enthalpy formulation integrated with fuel-air mixing



Challenges in applying conserved-scalar methods to multiple sources

- Subgrid parameter space: multiple conserved scalars, enthalpy, etc.
- Slowly evolving variables use progress variables: enthalpy-deficit, soot.
- Dissipation connects scales: differing length-scales, cross-dissipation
- Joint PDF evolution, marginal PDF independence

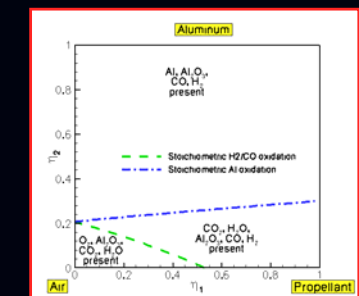
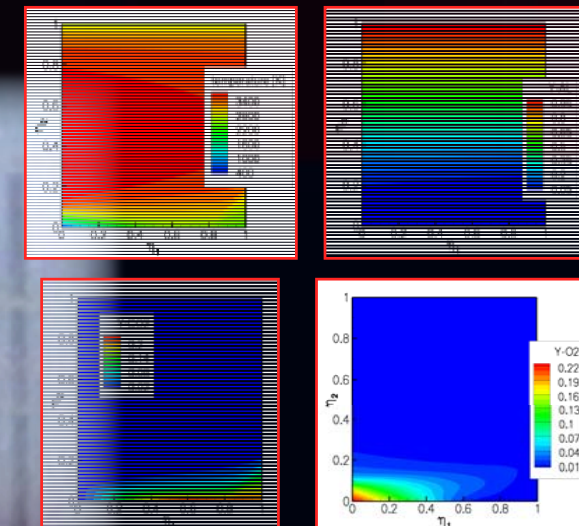
Issue: Al particles release substantial heat, but this varies in propellant fires with oxidizer



Accomplishment: new subgrid particle oxidation model treating multiple oxidizers through oxidizer-mixing conserved scalar.



Resolved subgrid thermochemical state for aluminum oxidation.



Range of Applications

- Multiple fuels (liquids, solids), oxidizers (propellants, air).
- Combined heat transfer and reacting flow.
- Other species (fire suppressants, contaminants).



Simulating the Pervasive Failure of Structures

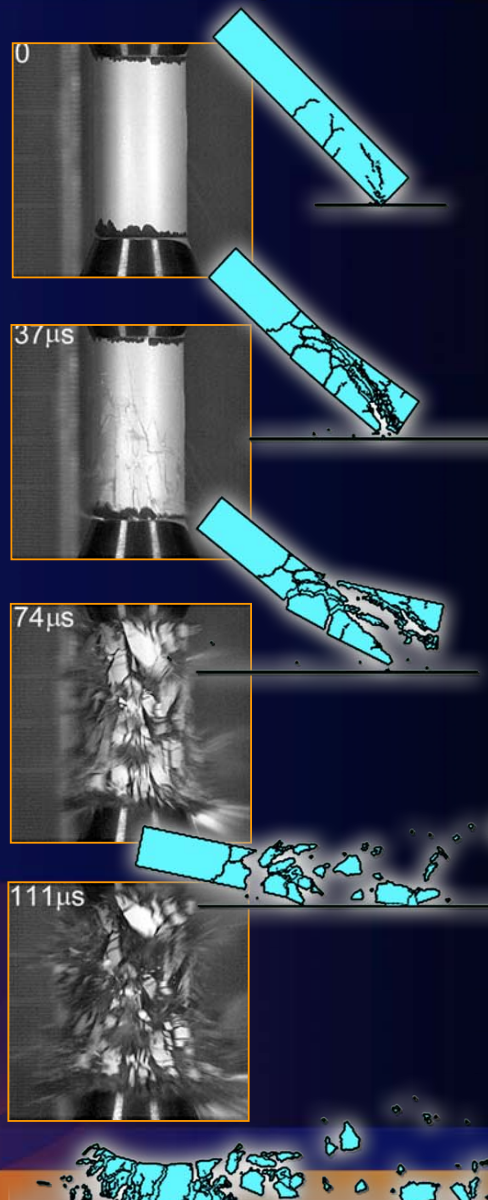
Joseph E. Bishop (1525)

Develop computational methods for simulating the dynamic failure of materials and structures.

ESRF Objectives:

- Develop a pure Lagrangian method for modeling the progression of a continuum to a discontinuum.
- Almost arbitrary crack nucleation, growth, branching and coalescence
- Method should be “convergent” with mesh refinement
- Application regimes from quasistatic single-crack growth to fragmentation.

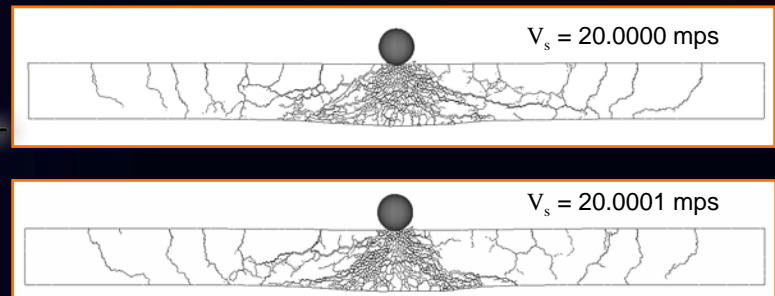
Impact and Fragmentation



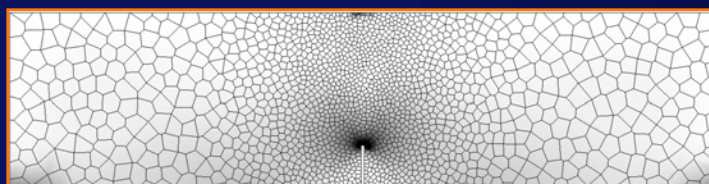
Computational Approach:

- Randomly close-packed Voronoi mesh
- Total-Lagrangian explicit dynamics
- Dynamic insertion of cohesive tractions
- Initially focus on quasibrittle materials, e.g. concrete

Sensitivity to Initial Conditions



Three-Point Bend



randomly close-packed Voronoi mesh



mid notch



offset notch

- Pervasive failure problems are extremely sensitive to initial conditions and system parameters (transient chaos)
- Use a weaker notion of mesh convergence: *convergence in probability*

$$\lim_{h \rightarrow 0} \Pr(P_h(q) - P(q) > \epsilon) = 0$$

h = mesh size
 q = engineering quantity of interest
 P = probability distribution



Hybrid Reynolds-Averaged Navier-Stokes/Large Eddy Simulation Models for Unsteady Turbulent Flows

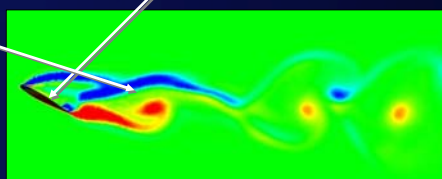
Matthew Barone (1515)

Abstract: Computational Fluid Dynamics (CFD) approaches that rely on finding steady solutions to averaged equations are often inadequate to accurately predict engineering properties of complex, separated, turbulent flows. Hybrid RANS/LES methods provide a promising avenue for improvement of CFD predictions for this class of flows. This research was aimed at evaluating currently available hybrid models, improving on the models and the numerics used to solve them, and validating the resulting simulation techniques over a range of aerodynamic applications of interest to Sandia and the broader research community.

Development and Evaluation of Hybrid Turbulence Models

Basic idea: apply quasi-steady RANS turbulence model in regions of attached flow and an unsteady LES model in regions of separated flow.

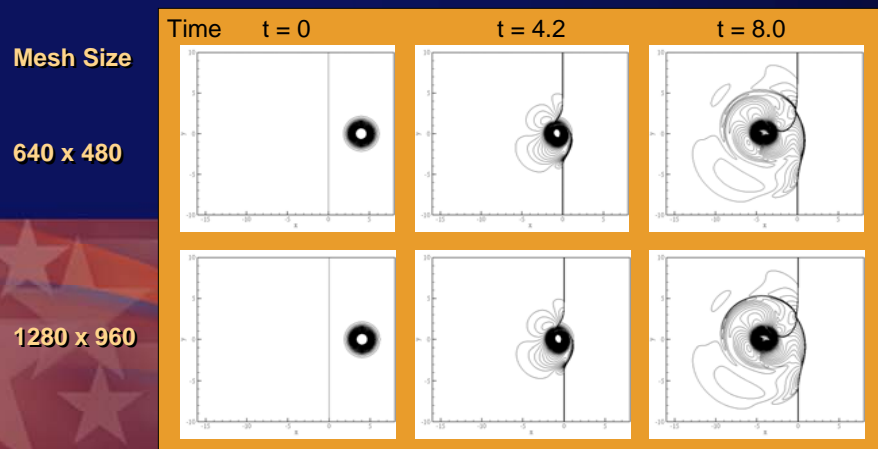
- Detached Eddy Simulation (DES) (P. Spalart)
 - Most widely used hybrid model, RANS and LES regions defined by the grid properties.
- Partially-Averaged Navier-Stokes (PANS) (S. Girimaji)
 - Allows for specification of a grid-independent LES filter width.
 - Developed in part as a collaboration with this research project.



Development and Verification of Non-dissipative Numerical Schemes

A key contribution of this research was development and testing of non-dissipative finite volume methods that mitigate the "smearing" of turbulent eddies by numerical dissipation, yet maintain numerical stability in the presence of shock waves.

Simulation of a vortex passing through a Mach 1.2 shock wave using a low-dissipation numerical scheme. As shown, the coarse mesh solution is nearly mesh-converged, whereas a conventional shock-capturing scheme requires at least twice as many mesh points in each dimension for comparable level of accuracy.

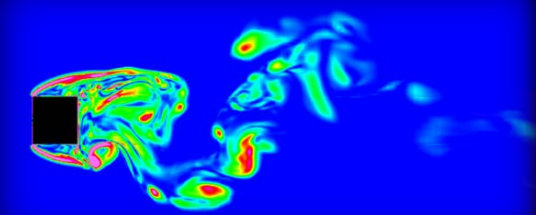


Publications:

- M. Barone and C.J. Roy, "Evaluation of Detached Eddy Simulation for Turbulent Wake Applications," *AIAA J.*, 44(12):3062-3071, 2006.
- M. Barone, "Mesh-independent unsteady turbulent wake simulations using the PANS model," *AIAA Paper 2006-3742*, 36th AIAA Fluid Dynamics Meeting, San Francisco, CA, June 5-8, 2006.

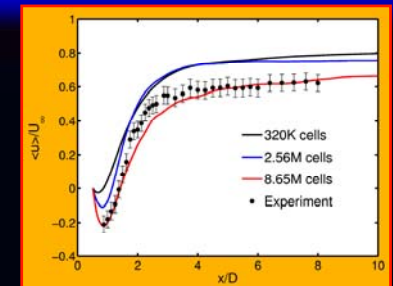
Validation: Low-speed Flow Past a Square Cylinder at $Re_D = 21,000$

Summary: The DES and PANS models were used to simulate flow past a square cylinder on several meshes with varying degrees of mesh refinement. The results were compared to experimental data for both mean and fluctuating quantities, indicating that for sufficient mesh resolution good agreement can be obtained.



Instantaneous snapshot of the vorticity magnitude in a cross-section of the cylinder wake.

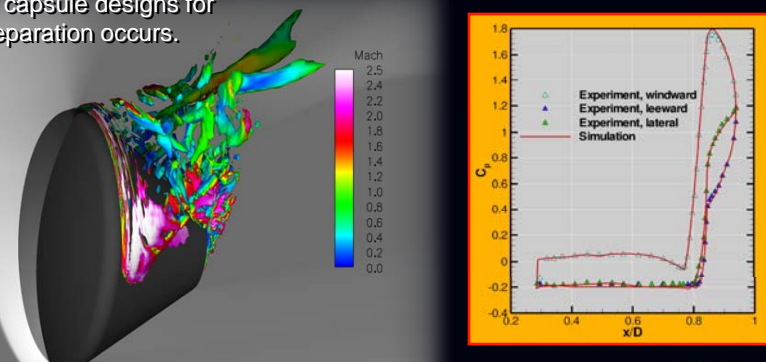
Comparison of the simulation results on several mesh levels with experimental data for the averaged stream-wise velocity along the wake centerline.



Application: Supersonic Flow Past a Space Capsule During Atmospheric Entry

Summary: Detached Eddy Simulations are being used to help NASA researchers define the aerodynamic properties of space capsule designs for flow conditions where massive separation occurs.

Comparison of computed time-averaged surface pressure coefficients with experimental data from the NASA Ames wind tunnel.



Instantaneous flow field of a re-entering space capsule at Mach number of 2.5. The greyscale pressure contours reveal the steady bow shock, while the isosurface of Q (vortex locator), colored by Mach number, shows a complex turbulent wake.



Enhanced Molecular Dynamics for Simulating Thermal and Charge Transport Phenomena in Metals and Semiconductors (09-1281)

Reese Jones (8776)

Project Summary

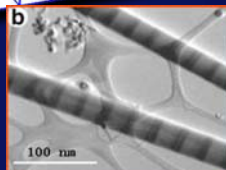
Problem: MD represents phonons and defects but not the electronic thermal & charge transport important in ICs, thermoelectrics, nanowire devices, etc.

Solution: Enhance MD with coupled and coincident FE-based hydrodynamic electron transport models.

Goal: To simulate electron-phonon exchange, Joule heating & thermopower effects on the nanodevice scale.

Significance: This project is extending a fundamental tool of material science & enabling a whole new class of predictive simulations, & nanoscale device design e.g. heat transport in defected metals under powered conditions

Pulse of energy superposed on a coupled FE/MD system



Ge/Si superlattice nanowires
[Dresselhaus, MIT]

First principles calculation of electron-phonon coupling

Unlike electron & phonon thermal conductivity & heat capacity, the electron-phonon coupling coefficient g is neither readily measured or calculated.

Three methods were explored:

- An integral over electron-phonon coupling coefficients obtained to first order from perturbation
- Using Green-Kubo relations and the density-density correlations
- Time-dependent Density Functional Theory (TDDFT) simulation of the transient relaxation of electron energy to the ion cores

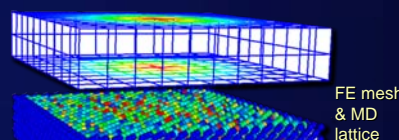
We are primarily using TDDFT, since unlike the first two methods TDDFT is not based on perturbation theory



Algorithm

Replace empirical phonon transport with MD to add:

- Phonon-confinement
- Ballistic transport
- Defect & grain boundary scattering



(1) Two temperature model (TTM):

storage diffusion exchange source

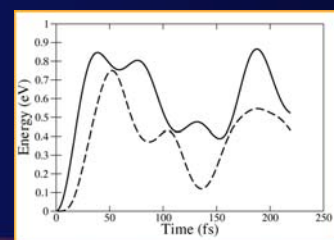
$$\text{electron: } \rho_e c_e \dot{T}_e = -k_e \nabla^2 T_e - g(T_e - T_p) + r_e$$

$$\text{phonon: } \rho_p c_p \dot{T}_p = -k_p \nabla^2 T_p - g(T_p - T_e)$$

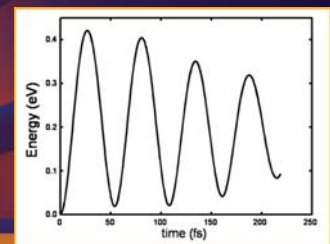
$$\text{MD: } \left\{ \begin{array}{l} m\dot{v} = f - \lambda \\ T_p = 1/3k \langle mv^2 \rangle \end{array} \right.$$

(2) Drift-diffusion model: driven by electrical potential (*drift*), & includes TTM effects (*diffusion*)

(3) Hydrodynamic model: high density of "hot" electrons, convection, & closest to Boltzmann transport



Evolution of the energies of the electronic state (solid) & Born-Oppenheimer ground state (dashed)



Difference energy, showing mean relaxation over time

Timescales

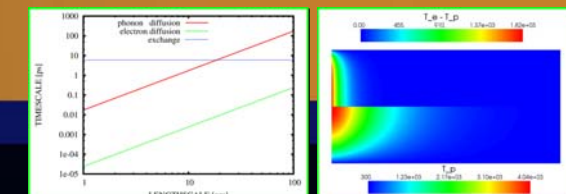
The TTM has three intrinsic timescales which are typically disparate & vary for different materials

Intrinsic timescales:

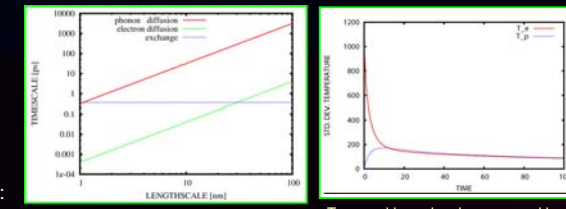
$$\text{Phonon diffusion: } \tau = \frac{L^2 c_p}{k_p}$$

$$\text{Electron diffusion: } \tau = \frac{L^2 c_e}{k_e}$$

$$\text{Electron-phonon Exchange: } \tau = \frac{c_e c_p}{g(c_e + c_p)}$$



Spatial boundary layer setup by injection of hot electrons (upper half) & diffusion of heat (lower half)

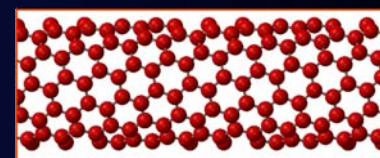
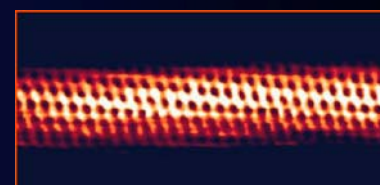


Temporal boundary layer caused by fast electron diffusion & electron-phonon exchange followed by slow phonon diffusion

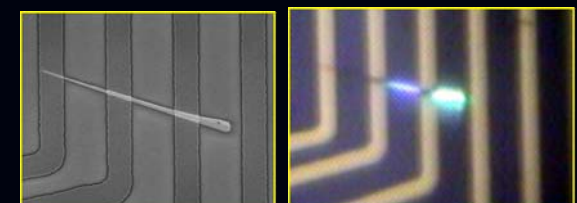
MD/FE Simulations of laser & Joule heating

We now have the capability to simulate of non-equilibrium processes like the relaxation after laser heating & quasi-steady Joule heating.

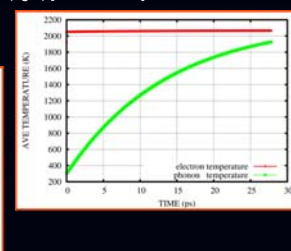
We are leveraging Ed Webb's work on a related LDRD: *Developing a thermal microscopy platform for in-situ thermal/thermoelectric structure-property studies of individual nanotubes and nanowires*



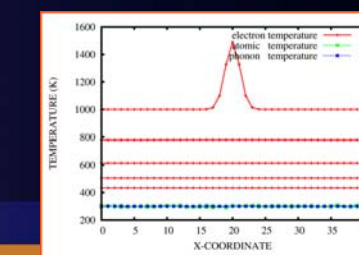
Carbon nanotube (CNT) image [TU Delft] & lattice



GaN nanowire under power and showing photoluminescence (right) [A. Talin, SNL]



Joule heating of a Cu nanowire showing fast response of the electron system and slower equilibration of the phonon system



CNT response to an initial Gaussian pulse

Multi-Length Scale Algorithms for Failure Modeling in Solid Mechanics

Benjamin Spencer, Martin Heinstein, Jason Hales

Computational Solid Mechanics & Structural Dynamics Department, Sandia National Laboratories, Albuquerque, NM

Introduction

Explicit transient dynamics is a widely used technique to solve solid mechanics problems, especially those involving highly nonlinear behavior, as is encountered in failure modeling. Although explicit time integration is an extremely powerful numerical technique, its applicability to problems that span length scales is limited because of the stability limits on the time step. The critical time step is controlled by the shortest time for a wave to traverse an element, which means that highly refined meshes require extremely small time steps.

The mechanical failure response of large systems is often governed by the behavior of details such as welds that have a length scale much smaller than that of the overall system. It is important to include these features in the model to capture the stress gradients associated with them, but including them in the model can come at a huge computational cost due to their effect on the critical time step.

A multi-length scale technique to address this problem is presented here. A coarse representation of the model is used in conjunction with the actual detailed finite element model of the structure. Explicit time integration is used to integrate the solution on the coarse mesh, so that the coarse mesh controls the temporal discretization, while the fine mesh controls the geometric discretization of the model.

Methodology

The standard dynamic equilibrium equation used to compute the acceleration, a , in explicit dynamics appears as:

$$Ma = R,$$

where M is the diagonal mass matrix and R is the residual obtained from summing external and internal forces. If a is the acceleration on the actual solution mesh, it can be represented as a summation of a high frequency component, a_{hf} on the fine mesh, and a low frequency component, a_{lf} on a coarse mesh. If Φ is an interpolation matrix, this can be expressed as:

$$a = a_{lf} + \Phi a_{hf}$$

The high and low frequency components of the response must be orthogonal. The following orthogonality condition is imposed:

$$a_{lf} \Phi^T M a_{hf} = 0$$

Decomposing the response in this manner leads to the following equation for the acceleration decomposed into low and high frequency components:

$$a = \Phi M_c^{-1} \Phi^T R + M^{-1} (R - M \Phi M_c^{-1} \Phi^T R)$$

where M_c is the mass on the coarse mesh, and is computed as:

$$M_c = \Phi^T M \Phi$$

Figure 1 demonstrates graphically this decomposition of the response into low and high frequency components.

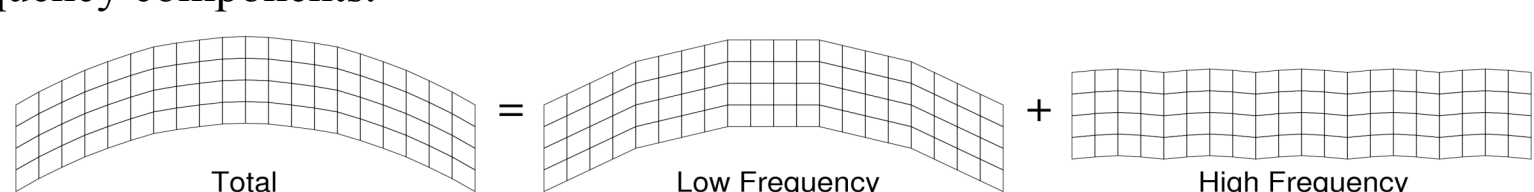


Figure 1. Decomposition of response into low and high frequency components

Up to this point, no approximations have been made in the solution. Decomposing the solution in this manner also would not affect the critical time step. To increase the critical time step, we can introduce a diagonal matrix, α , which contains mass scaling factors to be applied to the mass. The mass scaling factors are computed such that the critical time step of the high frequency response matches the larger critical time step of the coarse mesh. The dynamic equilibrium equation then takes the form:

$$a = \Phi M_{hf}^{-1} \Phi^T R + (\alpha M)^{-1} (R - M \Phi M_{hf}^{-1} \Phi^T R)$$

By applying mass scaling only to the high frequency part of the response, this method does not sacrifice accuracy in the important low frequency part of the response that is typically of most interest.

Applications

Laser Weld Test

This modal decomposition technique has been applied to an analysis of an experimental model used to test laser welds connecting components of a weapons system. Figure 2a shows a finite element model of the test specimen, with an exploded view showing details of the laser weld. The cylindrical plug was designed to approximate the mass of a component in an actual weapon system. It is attached to a circular plate by laser welds that penetrate through 1/3 the thickness of the plate. The outer edge of this plate was attached to a testing apparatus that was used to drop the specimen with the cylinder in a horizontal configuration, and abruptly stop when the specimen hit the bottom. The abrupt landing of the test specimen caused the cylinder to rotate relative to the plate and caused extreme stresses in the laser weld, especially near the top and bottom of the cylinder.

The extreme spread in length scales important to the response of this model makes it computationally challenging. To capture the potential failure of weld material, the mesh in that zone must have the high degree of refinement shown in Figure 2a. This model was run using the explicit multi-length scale technique presented here using two different coarse meshes: a coarser representation of the model conforming to the geometry of the test specimen as shown in Figure 2b, and a regular coarse mesh generated of the bounding box of the problem domain as shown in Figure 2c. This method does not restrict the coarse mesh to conform to the boundary of the actual model. This is significant because it simplifies the procedure for generating the coarse mesh and allows for larger elements to be used in the coarse mesh, resulting in a larger critical time step.

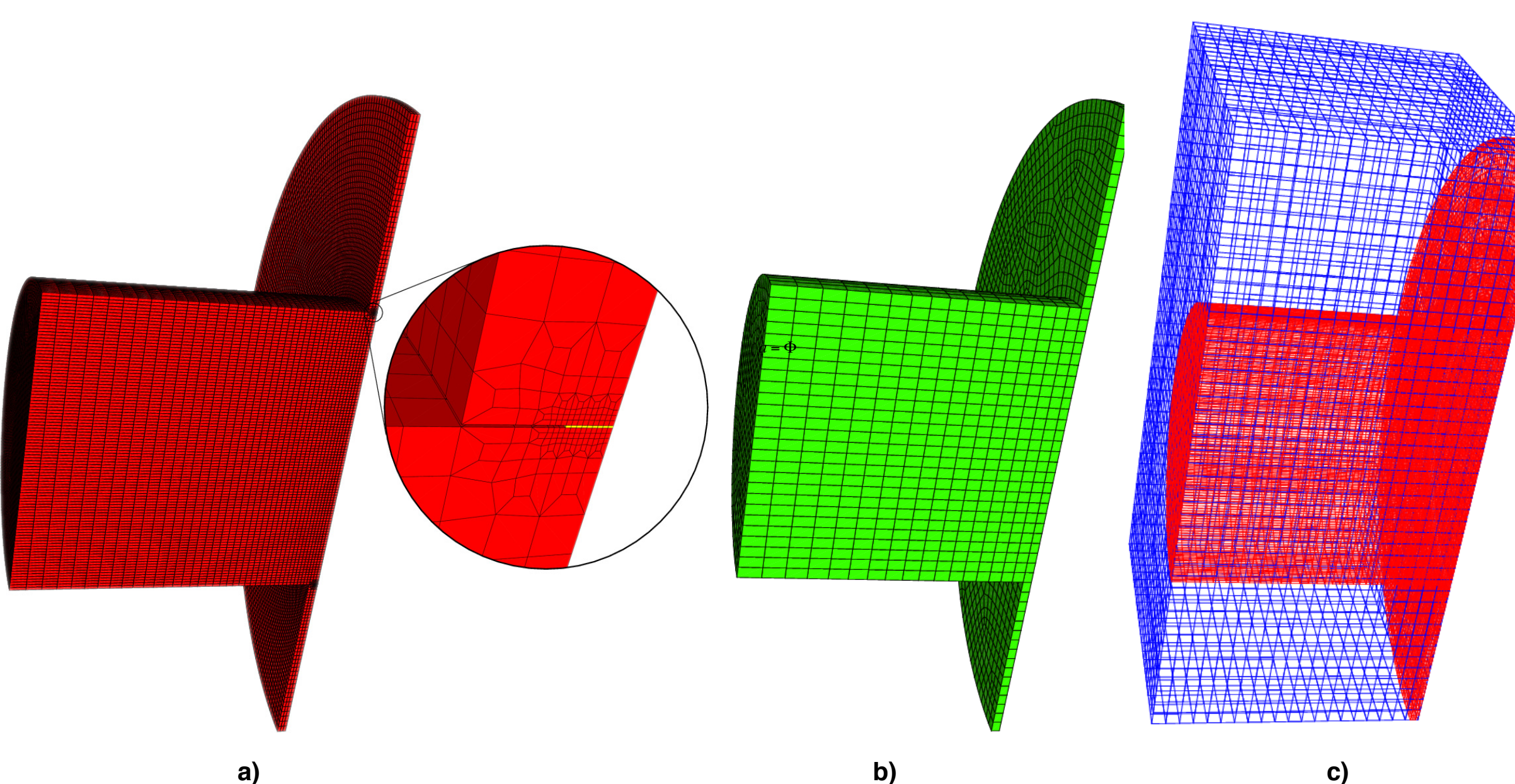


Figure 2. a) Finite element model of test specimen that approximates the actual physical characteristics of a weapon component. Detailed view shows how laser weld (yellow) penetrates through 1/3 of the plate thickness. b) Coarse mesh conforming to geometry of actual model mesh used for multi-length scale technique. c) Regular coarse mesh generated from bounding box of problem domain for multi-length scale technique. The coarse mesh is shown in blue, and the actual model mesh is shown in red.

Figure 3 shows the results of this analysis without the multi-length scale algorithm and using the two different coarse meshes. The results are very similar in all three cases, and in the best case, the multi-length scale technique resulted in a factor of 34 speedup.

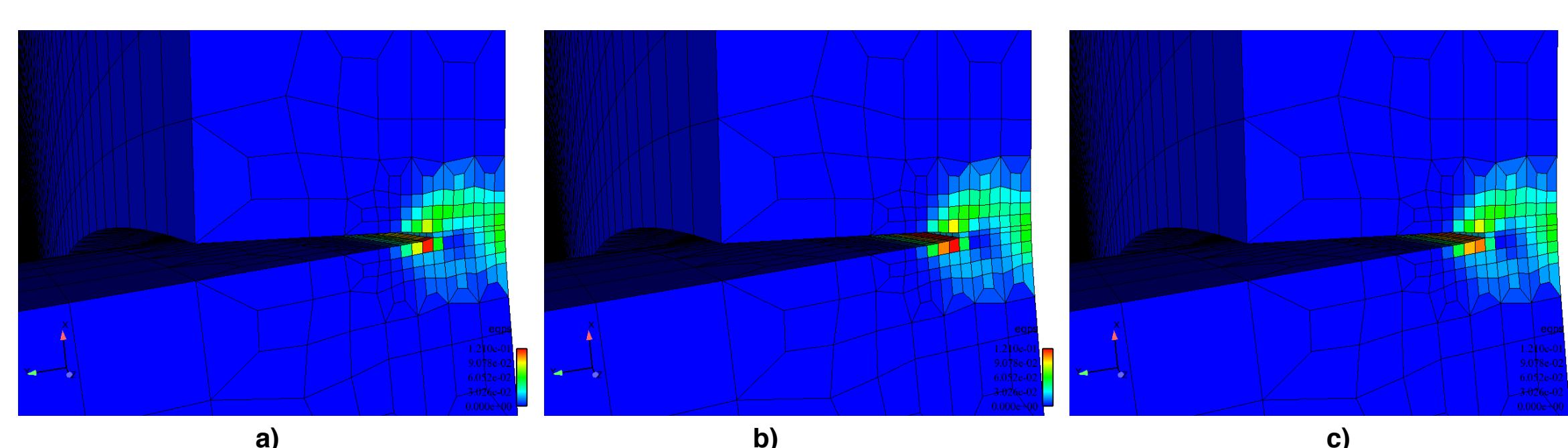


Figure 3. Plots of equivalent plastic strain shortly after weld failure initiation in zoomed-in region shown in Figure 2a. a) Results for baseline model using explicit time integration on fine mesh. Critical time step = 3.6e-9s, run time = 205m on 200 processors. b) Results using multi-length scale technique with coarse mesh shown in Figure 2b. Critical time step = 1.2e-7s, run time = 8m on 200 processors. c) Results using multi-length scale technique with coarse mesh shown in Figure 2c. Critical time step = 1.8e-7s, run time = 6m on 200 processors.

Applications

Plate Blast Problem

To demonstrate the effectiveness of this technique on problems with large deformations and pervasive failure, an analysis has been performed on a quarter-symmetry model of a plate subjected to a blast load. The actual mesh is shown in red along with the coarse mesh in Figure 4a. The results with and without the multi-length scale technique are shown in Figure 4b and 4c. The multi-length scale model had a 4.2x increase in the critical time step and a 2.2x decrease in run time.

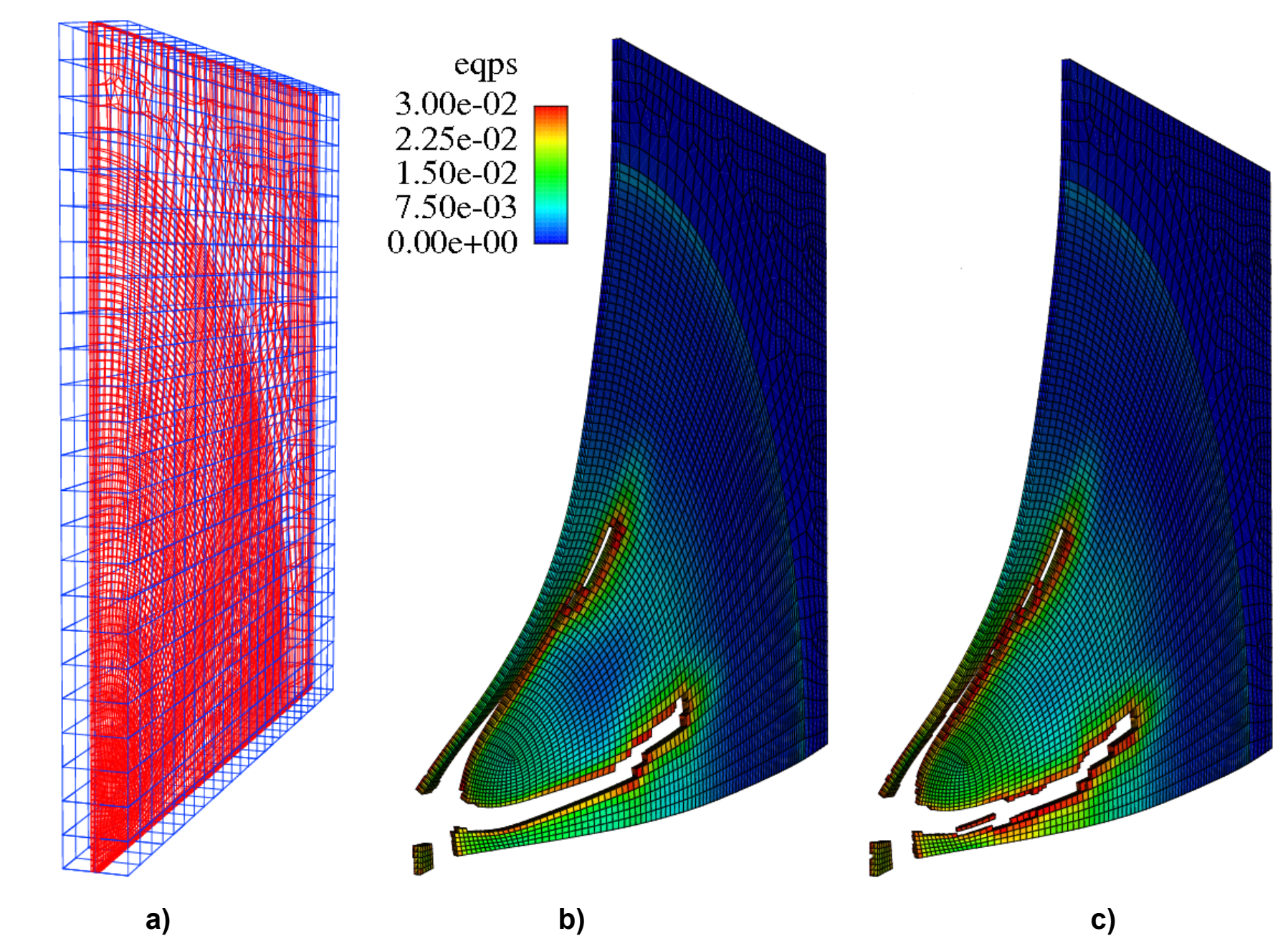


Figure 4. Finite element meshes and results for plate blast problem. a) Fine scale finite element model of plate (red) and coarse mesh (blue). b) Baseline results on fine model showing deformed mesh and equivalent plastic strain. c) Results for multi-length scale model showing deformed mesh and equivalent plastic strain.

Summary

A multi-length scale technique for explicit transient dynamics has been developed. This allows for a fine mesh to represent the geometric details of the model and capture the gradients necessary for the model to represent the important physics of the problem. The explicit time integration is carried out on a coarse mesh that overlays the fine mesh of the model.

An analyst using this technique can choose the mesh discretization of the fine mesh to properly represent the geometry and physics of interest, while choosing the coarse mesh to provide a satisfactory critical time step. This is in contrast to the current state of the art, where compromises in mesh resolution often need to be made to obtain a solution using a reasonable amount of computational resources.

The effectiveness and accuracy of this technique have been demonstrated on application problems. This technique has been shown to produce accurate results with a significant savings in computational cost.

